The 8th European Congress on Computational Methods in Applied Sciences and Engineering
ECCOMAS Congress 2022
5-–9 June 2022, Oslo, Norway

LOW MACH PRECONDITIONED NON-REFLECTING BOUNDARY CONDITIONS FOR THE HARMONIC BALANCE SOLVER

PIERRE SIVEL[1] AND CHRISTIAN FREY[2]

Institute of Propulsion Technology
German Aerospace Center (DLR)
Linder Höhe, 51147 Cologne, Germany
e-mail: [1]pierre.sivel@dlr.de, [2]christian.frey@dlr.de

Key words: Computational Fluid Dynamics, Low Mach Preconditioning, Harmonic Balance, Non-Reflecting Boundary Conditions

Abstract. In computational fluid dynamics (CFD), unsteady computations are cost-intensive. The Harmonic Balance (HB) method [7] represents a cost-efficient alternative. Here, for time-periodic flows, the governing equations are recasted in the Fourier domain.

In the low Mach regime, the compressible governing equations are stiff. Therefore, density-based solvers converge slowly. Low Mach preconditioning equalizes the eigenvalues of the system of equations, to improve the condition number and remove the stiffness of the system [14].

In this paper, low Mach preconditioning is applied to the HB method, with emphasis on the non-reflecting boundary conditions (NRBCs). These boundary conditions have a crucial impact on the flow inside the truncated computational domains used in CFD. Improper boundary conditions reflect waves exiting the computational domain and deteriorate the quality of the solution. However, NRBCs [6] avoid spurious reflections.

We explain that to precondition the NRBC its formulation in terms of characteristics has to be adapted. An academic wave propagation test case is computed for different wave configurations to validate the preconditioned boundary conditions.

The use of non-preconditioned NRBCs in a preconditioned computation leads to instabilities and reflections at the boundaries of the domain. A consistent setup with preconditioned NRBCs improves the stability and leads to good non-reflecting properties for all presented wave configurations.

1 INTRODUCTION

In the low Mach regime, the compressible Euler equations become stiff, because of the large discrepancy between the acoustic and convective eigenvalues. This means that computations of low Mach flows with density-based solver converge slowly [10]. Low Mach preconditioning is a method, which greatly improves the convergence by equalizing the eigenvalues of the system of equations.

It was first introduced by Chorin [3] for the incompressible Euler equations. Here, the author increased the coupling of the continuity equation by scaling its time derivative, thereby altering the compressibility of the system. Later, this method was further developed by several authors.

Choi and Merkle [10, 2] derived preconditioning matrices based on asymptotic analysis of the governing equations for low Mach numbers, Turkel et al. [14] proposed matrices for the compressible equations based on the original method proposed by Chorin, and Van Leer et al [16] focused on the derivation of symmetrizable preconditioning matrices. All of these matrices were applied to steady state problems and showed a significant improvement of the convergence in the low Mach regime.

Venkateswaran and Merkle [17] applied the method to unsteady flow. Here, a dual-time stepping approach was used. This allowed to precondition the pseudo-time derivative of the equations instead of the physical time derivative. This way the temporal accuracy of the solution in the physical time is preserved. Further, they showed that to optimize the convergence, the preconditioning matrix must be a function of the physical time step. This approach was later applied successfully to a three dimensional rotorcraft flow by Potsdam et al. [11].

In this work, low Mach preconditioning is applied to the HB method. HB is an efficient method to solve time-periodic flows in the frequency domain [7, 5]. The time-domain governing equations are recasted by expressing the flow as Fourier coefficients about the fundamental frequency of the flow. This results in a non-linear system of equations for the Fourier coefficients of the state, which is solved as a steady state problem in the frequency-domain.

The first application of low Mach preconditioning for the HB method was presented by Howison and Ekici [8]. They computed wind turbine blade test cases, showing the improved convergence and accuracy of the preconditioned HB solver. Based on these results, Djeddi et al. [4] presented a preconditioner which fully incorporates the Spalart-Allmaras turbulence model to further improve the convergence.

The previous applications of low Mach preconditioning for the HB method focus on external flow computations. However, in internal flow computations the boundary conditions may need to be placed close to the area of interest. Therefore, improperly defined boundary conditions can lead to spurious reflection. To avoid reflections, Giles [6] proposed a steady state NRBC based on the decomposition of the boundary flow into modes, and the suppression of incoming modes. The NRBC was extended for three dimensional flow by Saxer et al. [12]. Schlüß et al. [13] proposed a spectral NRBC, which takes into account unsteady perturbations at the boundaries. A frequency domain application of the spectral NRBC was described by Kersken at al. [9]. Anker et al. [1] presented a preconditioned version of the NRBC proposed by Saxer et al. In this work, the spectral NRBC presented by Kersken et al. and by Schlüß et al. are preconditioned. Here, the boundary condition based on the modal decomposition of the flow state, is not influenced by low Mach preconditioning. However, the characteristic framework used to increase the robustness of the NRBC must be preconditioned to avoid spurious reflections.

In the first section of this paper, low Mach preconditioning is explained. Following that, the HB method is presented, including the application of low Mach preconditioning. Then, the preconditioned NRBC is described. Finally, a preconditioned wave propagation test case is computed with preconditioned and non-preconditioned NRBCs. The results show that the use of non-preconditioned NRBCs in a preconditioned computation results in stability issues and increased reflections at the outlet boundary. With preconditioned NRBCs, all computations remained stable and had good non-reflecting properties.

2 LOW MACH PRECONDITIONING

The discrepancy between the acoustic and convective eigenvalues of the Euler equations increases in the low Mach regime, which leads to a very stiff system of equations. Therefore, density-based solvers converge slowly, when solving low Mach flows. The goal of low Mach preconditioning is to remove the stiffness of the system, by equalizing its eigenvalues. This is achieved by multiplying the time derivative of the governing equations with a preconditioning matrix P^{-1}

$$P^{-1}\frac{\partial q}{\partial t} + \frac{\partial F}{\partial x} + \frac{\partial G}{\partial y} + \frac{\partial H}{\partial z} = 0. \tag{1}$$

Here, F, G and H are the convective fluxes in x, y and z direction, t is the time and q is the state vector.

In this work, the preconditioning matrix presented by Turkel [14] is used. It is defined in primitive entropy variables $q_S = (\rho, u, v, w, S)$, where ρ is the density, $U = (u, v, w)$ is the Cartesian velocity vector and S is the specific entropy. The preconditioning matrix reads

$$P_S = \mathrm{diag}\left(\beta^2, 1, 1, 1, 1\right). \tag{2}$$

Here, β^2 is the preconditioning parameter.

An indicator for the stiffness of a system of equations is its condition number

$$\kappa = \frac{|\lambda|_{\max}}{|\lambda|_{\min}}. \tag{3}$$

Here, λ_i are the eigenvalues of the systems flux Jacobian

$$PD = P\left(\frac{\partial F}{\partial q} + \frac{\partial G}{\partial q} + \frac{\partial H}{\partial q}\right). \tag{4}$$

Its eigenvalues are

$$\lambda_{1,2,3} = \sqrt{u^2 + v^2 + w^2} \tag{5}$$

$$\lambda_{4,5} = \frac{1}{2}\left(\left(\beta^2 + 1\right)\lambda_{1,2,3} \pm \sqrt{\left(1 - \beta^2\right)^2 \lambda_{1,2,3}^2 + 4\beta^2 a^2}\right). \tag{6}$$

Here, a is the isentropic speed of sound.

Choosing the preconditioning parameter to be $\beta^2 = 1$ disables the preconditioner and retrieves the non-preconditioned equations. In this case, the eigenvalues of the system are

$$\lambda_{1,2,3} = \sqrt{u^2 + v^2 + w^2} \tag{7}$$

$$\lambda_{4,5} = \lambda_{1,2,3} \pm a. \tag{8}$$

The Mach number is defined as

$$Ma = \frac{\sqrt{u^2 + v^2 + w^2}}{a}. \tag{9}$$

For Mach numbers tending to zero the condition number tends to infinity, demonstrating the stiffness of the non-preconditioned equations.

However, since the acoustic eigenvalues $\lambda_{4,5}$ depend on the preconditioning parameter, a value for the preconditioning parameter can be found that best equalizes the acoustic and convective eigenvalues. This optimal preconditioning parameter is $\beta^2 = Ma^2$. For Mach numbers tending to zero, this will lead to a finite condition number of $\kappa \approx 2.6$, effectively removing the stiffness of the system and improving the converge for low Mach flows.

3 HARMONIC BALANCE

Solving the unsteady Euler equations in the time-domain is cost-intensive. For time periodic flows, the HB method is a cost-efficient alternative. It is derived by expressing the unsteady state as a Fourier series about the fundamental frequency of the flow ω

$$q\left(t\right) = \mathrm{Re}\left(\sum_{k=0}^{\infty} \widehat{q}_k\left(x,y,z\right) e^{ik\omega t}\right). \tag{10}$$

Here, $\hat{q}_k$ is the Fourier coefficient of the k-th harmonic. The Fourier series is inserted into the governing equations, which leads to the non-linear system of equations.

$$ik\omega\widehat{q}_k + \widehat{R}_k(q) = 0, \quad \text{for} \quad k = 0,\ldots,K. \tag{11}$$

This system of equations is solved directly for the Fourier coefficients of the harmonics in the frequency-domain using standard steady state approaches. This reduces the computational cost compared to time-domain methods. Of course, these equations cannot be solved for an infinite number of harmonics. Instead, the unsteady state is approximated using a finite number of harmonics K.

Due to the non-linearity of the time-domain residual R, the Fourier coefficients of the residual $\widehat{R}_k(q)$ depend on all K harmonics of the state. The calculation of the non-linear residuals sets apart the different HB approaches. Here, an alternating time-domain frequency-domain method is used. In other words, the system of equations is solved in the frequency-domain, but the non-linear residual is calculated in the time-domain. At a finite number of equidistant sampling points in time, the unsteady state is reconstructed and the residual is calculated. Then, the harmonics of the residual are calculated with a discrete Fourier transform. The minimum number of sampling point is defined by the frequency of the highest harmonic and the Nyquist criteria.

We apply low Mach preconditioning to the HB equations (11) as presented in the previous section. However, since we do not want to change the solution of the original system, a pseudo-time marching scheme is used to solve the system of equations and the pseudo-time derivative is preconditioned

$$P^{-}1\frac{\partial\hat{q}_k}{\partial\tau} + ik\omega\widehat{q}_k + \widehat{R}_k(q) = 0, \quad \text{for} \quad k = 0,\ldots,K. \tag{12}$$

Regarding the preconditioning parameter, the same value is used for all harmonics. Here, the average Mach number is used, which corresponds to the zeroth harmonic of the Mach number

$$\beta^2 = \widehat{Ma}_0^2. \tag{13}$$

4 PRECONDITIONED NON-REFLECTING BOUNDARY CONDITIONS

In this section, the two-dimensional NRBC presented by Kersken et al. [9] is adapted for low Mach preconditioned computations. The preconditioning method is equally applicable to the unsteady time-domain version of the NRBC presented by Schlüß et al. [13].

The NRBC is derived based on two assumptions. The first is that the flow is inviscid and that perturbations from the mean flow are small. The second assumption is that the flow is dominated by two-dimensional effects. This means that perturbations in radial direction

for rotational configurations and in z-direction for translational configurations are negligible. Therefore, the NRBC can be based on the unsteady two-dimensional linear equations

$$\frac{\partial q'}{\partial t} + A\frac{\partial q'}{\partial x} + B\frac{\partial q'}{\partial y} = 0. \tag{14}$$

They are formulated using the primitive state $q = (\rho, u, v, w, p)$, which is separated into an average flow $\bar{q}$ and perturbations around the average flow q' by $q = \bar{q}+q'$. The NRBC is computed in the reference system of the boundary. In other words, x is defined in boundary normal direction. For translational cases, the y-coordinate is defined by the Cartesian y-direction. However, for rotational configurations, y denotes the circumferential coordinate, which is defined by $y = r\phi$, where r is the radius and ϕ is the pitch. The velocity components u and v are defined accordingly in x and y direction. The primitive flux Jacobians of the linearized Euler equations are

$$A = \begin{pmatrix} \bar{u} & \bar{\rho} & 0 & 0 & 0 \\ 0 & \bar{u} & 0 & 0 & 1/\bar{\rho} \\ 0 & 0 & \bar{u} & 0 & 0 \\ 0 & 0 & 0 & \bar{u} & 0 \\ 0 & \bar{\rho}\bar{a}^2 & 0 & 0 & \bar{u} \end{pmatrix} \quad \text{and} \quad B = \begin{pmatrix} \bar{v} & 0 & \bar{\rho} & 0 & 0 \\ 0 & \bar{v} & 0 & 0 & 0 \\ 0 & 0 & \bar{v} & 0 & 1/\bar{\rho} \\ 0 & 0 & 0 & \bar{v} & 0 \\ 0 & 0 & \bar{\rho}\bar{a}^2 & 0 & \bar{v} \end{pmatrix}. \tag{15}$$

The perturbations in the flow can be expressed has a superposition of wave-like solutions

$$q' = \mathrm{Re}\left(\hat{q}e^{i(kx+ly+\omega t)}\right). \tag{16}$$

These wave are defined by a non-zero amplitude $\hat{q}$, an angular frequency ω and the wave numbers k and l along the x and y directions, respectively. We insert this solution into the linearized equations (14), which simplifies to the dispersion relation

$$\det\left(\omega I + kA + lB\right) = 0, \tag{17}$$

For a given combination of ω and l, the dispersion relation is an eigenvalue problem with five eigenvalues corresponding to the negative axial wave numbers $-k$. For each mode, i.e. for every combination of ω and l, the dispersion relations leads to the set of eigenvalues:

$$k_{1,2,3} = -\frac{l\bar{v}+\omega}{\bar{u}} \tag{18}$$

$$k_{4,5} = \frac{l\bar{v}+\omega}{\bar{a}^2-\bar{u}^2}\left(\bar{u} \mp \Phi\right), \tag{19}$$

with

$$\Phi = \begin{cases} \sqrt{\Delta}, & \text{if} \quad \Delta \geq 0 \\ -i\mathrm{sign}\left(l\bar{v}+\omega\right)\sqrt{-\Delta}, & \text{if} \quad \Delta < 0 \end{cases} \tag{20}$$

and

$$\Delta = \bar{a}^2\left(1 + \frac{l^2\left(\bar{u}^2-\bar{a}^2\right)}{\left(l\bar{v}+\omega\right)^2}\right). \tag{21}$$

Definition (20) ensures that for subsonic flows the waves corresponding to the first four eigenvalues are propagating downstream and the wave corresponding to the fifth eigenvalue is always propagating upstream. The five right eigenvectors corresponding to each eigenvalue in (18), form the right eigenvector matrix

$$R = (r_1, r_2, r_3, r_4, r_5) = \begin{pmatrix} -\bar{\rho} & 0 & 0 & \bar{\rho} & \bar{\rho} \\ 0 & \bar{a}\bar{u}l & 0 & -\frac{\bar{a}^2 k_4}{(\omega + l\bar{v} + k_4\bar{u})} & -\frac{\bar{a}^2 k_5}{(\omega + l\bar{v} + k_5\bar{u})} \\ 0 & \bar{a}\left(\omega + l\bar{v}\right) & 0 & -\frac{\bar{a}^2 m}{(\omega + l\bar{v} + k_4\bar{u})} & -\frac{\bar{a}^2 m}{(\omega + l\bar{v} + k_5\bar{u})} \\ 0 & 0 & \bar{a} & 0 & 0 \\ 0 & 0 & 0 & \bar{\rho}\bar{a}^2 & \bar{\rho}\bar{a}^2 \end{pmatrix}. \tag{22}$$

Here, each eigenvector describes a fundamental wave. The first eigenvector r_1 corresponds to an entropy wave, the second eigenvector r_2 and the third eigenvector r_3 represent vorticity waves in radial and circumferential direction and the fourth eigenvector r_4 and the fifth eigenvector r_5 constitute downstream and upstream acoustic waves, respectively.

The amplitude of every mode $\hat{q}_{\omega,l}$ is a linear combination of these right eigenvectors

$$\hat{q}_{\omega,l} = \sum_{i=0}^{5} \alpha_i r_i. \tag{23}$$

The modal transformation which decomposes each mode into the fundamental waves is the left eigenvector matrix $L = (l_1, l_2, l_3, l_4, l_5)^T = R^{-1}$. Therefore, the weight of each right eigenvector in (23) is defined as

$$\alpha_i = l_i \hat{q}_{\omega,l}. \tag{24}$$

To enforce a non-reflecting behavior at the boundaries, we allow outgoing waves to exit the domain, but suppress all incoming waves. This is achieved by setting the weights of incoming waves to zero, which results in the non-reflecting boundary condition

$$L^{\text{inc}} \hat{q}_{\omega,l} = 0. \tag{25}$$

Here, L^{inc} is the matrix containing the left eigenvectors corresponding to incoming modes.

In some cases, we need to prescribe incoming modes at the boundaries of the domain. This is achieved by defining the desired non-zero value for the incoming modal amplitude. This changes the NRBC to

$$L_{\text{inc}} \left(\hat{q}_{\omega,l} + \hat{q}^{\text{bd}}_{\omega,l} \right) = 0, \tag{26}$$

where $\hat{q}^{\text{bd}}_{\omega,l}$ is the user defined modal amplitude.

This boundary condition (25) is purely based on physical properties of the linearized flow. Therefore, it remains unaffected by low Mach preconditioning. However, an application of the NRBC based on modes, may not be well-posed in the pseudo-time, which leads to instabilities [9, 13]. A more robust approach is to apply the NRBC using a frame-work of one-dimensional characteristics, which are known to be well-posed [6]. Here, the characteristics must be properly

defined in the pseudo-time. Since the pseudo-time has been preconditioned in (12), the framework must be based on the preconditioned characteristics. These are derived by computing the dispersion relation (17) for a preconditioned one dimensional wave.

$$det\left(I\omega + PAk\right) = 0. \tag{27}$$

solving the dispersion relation leads to the preconditioned right eigenvector matrix

$$R_{1D} = \begin{pmatrix} -\bar{\rho} & 0 & 0 & \bar{\rho}\beta^2 & \bar{\rho}\beta^2 \\ 0 & 0 & 0 & \left(\bar{\lambda}_4 - u\beta^2\right) & \left(\bar{\lambda}_5 - \bar{u}\beta^2\right) \\ 0 & \bar{a} & 0 & 0 & 0 \\ 0 & 0 & \bar{a} & 0 & 0 \\ 0 & 0 & 0 & \bar{\rho}\beta^2\bar{a}^2 & \bar{\rho}\beta^2\bar{a}^2 \end{pmatrix}. \tag{28}$$

Here, $\bar{\lambda}_i$ are the preconditioned eigenvalues (5) based on the average flow. This right eigenvector matrix and its inverse $L_{1D} = R_{1D}^{-1}$ are the transformation matrices between the primitive q and characteristic state c

$$L_{1D}\hat{q} = \hat{c} \quad \text{and} \quad R_{1D}\hat{c} = \hat{q}. \tag{29}$$

Here, analogously to the fundamental waves, the first four eigenvectors of R_{1D} correspond to downstream characteristics and the fifth eigenvector to an upstream characteristic.

The boundary condition is now applied in terms of preconditioned characteristic variables. Thanks to the mixed time-domain frequency-domain implementation of the HB method, the NRBC is applied directly in the frequency domain. Therefore, the starting point is the primitive temporal Fourier state $\hat{q}_\omega$ for each computed harmonic. First, the modal amplitudes $\hat{q}_{\omega,l}$ are computed by means of a Fourier decomposition in circumferential direction for rotational cases or in y-direction for translational cases. Then the modes are transformed into characteristics $\hat{c}_{\omega,l}$ following (29). For each mode, the NRBC (25) is expressed in terms of characteristics

$$L^{\text{inc}}(\omega,l)\hat{q}_{\omega,l} = 0 = L^{\text{inc}}(\omega,l)\left(R_{1D}^{\text{inc}}\hat{c}_{\omega,l}^{\text{inc}} + R_{1D}^{\text{out}}\hat{c}_{\omega,l}^{\text{out}}\right) \tag{30}$$

and is solved for a target incoming characteristic

$$\hat{c}_{target,\omega,l}^{\text{inc}} = -\left(L^{\text{inc}}(\omega,l)R_{1D}^{\text{inc}}\right)^{-1} L^{\text{inc}}(\omega,l)R_{1D}^{\text{out}}\hat{c}_{\omega,l}^{\text{out}}, \tag{31}$$

which ensures a non-reflective behavior for this mode. Here, the superscripts "inc" and "out" denote all entries associated with incoming or outgoing characteristics and modes. The target incoming characteristic is a function of the outgoing, which are extrapolate form the inner cell. To increase the stability, the target characteristics are relaxed, leading the updated characteristics

$$\hat{c}_{\omega,l} = \sigma\hat{c}_{target,\omega,l} + (1-\sigma)\,\hat{c}_{previous,\omega,l}. \tag{32}$$

The relaxation factor σ is usually set to 0.1.

For the average mode, i.e. $\omega = 0$ and $l = 0$, the NRBC (25) is not applied. Instead this mode is used to enforce the user-defined boundary values. This is achieved by driving the residual

$$\mathcal{R} = \mathcal{R}_{\text{bd}}^{\text{inc}} + \mathcal{R}_{\text{i}}^{\text{out}} \tag{33}$$

to zero. The residuals are defined as

$$\mathcal{R}_{\mathrm{bd}} = \begin{pmatrix} \bar{p}\left(\bar{s} - s^{\mathrm{bd}}\right) \\ \bar{\rho}\bar{a}\left(\bar{v} - \bar{u}\tan\left(\alpha_{circ,\mathrm{bd}}\right)\right) \\ \bar{\rho}\bar{a}\left(\bar{w} - \bar{u}\tan\left(\alpha_{rad,\mathrm{bd}}\right)\right) \\ \bar{\rho}\left(\bar{h}_t - h_{t_{\mathrm{bd}}}\right) \\ \bar{p} - p^{\mathrm{bd}} \end{pmatrix} \quad \text{and} \quad \mathcal{R}_i = L_{1D}\left(\bar{q}_{\mathrm{f}} - \bar{q}_{\mathrm{i}}\right). \tag{34}$$

Here, the subscript "bd" denotes the user defined boundary values and the subscripts "i" and "f" denote the face state and the inner first cell state. The update of the average characteristics is calculated with one Newton-Raphson step each pseudo-time iteration

$$\mathcal{R} + \frac{\partial \mathcal{R}}{\partial c}\delta\bar{c} = 0. \tag{35}$$

With $\mathcal{R}_{\mathrm{bd}}^{\mathrm{inc}}$ and $\mathcal{R}_{\mathrm{i}}^{\mathrm{out}}$ driven to zero, the incoming characteristic enforce the prescribed boundary values, while the outgoing characteristics are extrapolated from inside the computational domain. The updated average characteristic is then calculated as

$$\hat{c}_{0,0,new} = \hat{c}_{0,0} + \sigma_{\mathrm{av}}\delta\bar{c} \tag{36}$$

Here, σ_{av} corresponds to the relaxation factor σ, but it is only applied to incoming characteristics.

The updated characteristics are transformed back to temporal characteristics $\hat{c}_\omega$ using an inverse Fourier transform and, finally, they are transformed into the new primitive state $\hat{q}_\omega = L_{1D}\hat{c}_\omega$ for each harmonic.

5 RESULTS

A circular duct with prescribed two-dimensional waves is computed with the preconditioned HB solver. The duct is 0.0125 m long and has a radius of 1 m. The computed section is a 400th of the full annulus. The domain is discretized with 128 cells in axial direction, 64 cells in circumferential direction and a single cell in radial direction. The boundaries in radial direction are inviscid walls and in axial direction NRBCs are applied for the inflow and the outflow. In circumferential direction the flow is periodic.

The inviscid flow in the duct is computed, by solving the Euler equations. A preconditioned Roe scheme for unsteady flow is used to discretize the convective fluxes [11]. Second order accuracy in space is obtained with a MUSCL scheme [15]. The equations are solved implicitly with an Euler backwards scheme for the pseudo-time. The implicit system is solved with a Gauß-Seidel algorithm. All computations are preconditioned.

At the inflow, a stagnation temperature of 350 K and a stagnation pressure of 100 000 Pa are prescribed as boundary values. At the outlet, the static pressure is set to 99 990 Pa. This

Table 1: Stability for different prescribed waves computed with the preconditioned HB solver with preconditioned and non-preconditioned NRBC.

	acoustic	vorticity	entropy
non-preconditioned NRBC	no convergence	unstable	unstable
preconditioned NRBC	converged	converged	converged

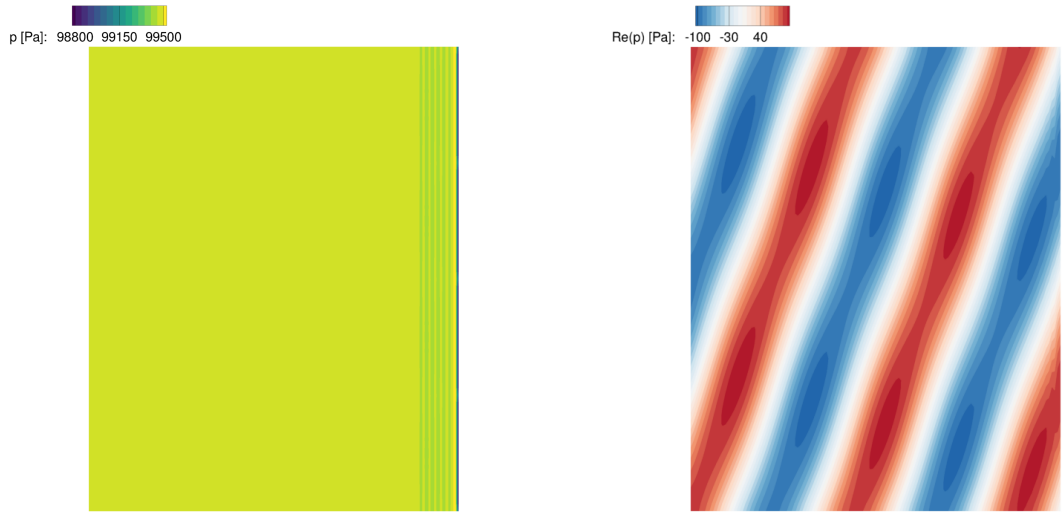

(a) zeroth harmonic (b) first harmonic

Figure 1: Solution for an acoustic wave computed with the preconditioned HB solver with non-preconditioned NRBC.

results in an average Mach number of $\widehat{Ma}_0 = 0.012$. All HB computations are initialized with a converged steady state solution, computed with the described boundary values.

The test case is computed for three different waves prescribed at the inflow: A downstream acoustic wave, a entropy wave and a vorticity wave. All waves have a circumferential wave number of $l = 400$. For the acoustic wave, the frequency is $f = 78\,531.37\,\mathrm{Hz}$ and the amplitude corresponds to a $100\,\mathrm{Pa}$ pressure perturbation. The vorticity wave and the entropy wave are transported at the convective speed. Therefore, to maintain the same axial wave number as for the acoustic wave, the frequency is reduced to $f = 940\,\mathrm{Hz}$. The amplitude of the entropy wave corresponds to a temperature perturbation of $1\,\mathrm{K}$ and the amplitude of the vorticity wave corresponds to a perturbation of the axial velocity of $1 \times 10^{-3}\,\mathrm{m/s}$. The flow is computed using only the zeroth and the first harmonic of the waves' frequencies.

In a first step, we will demonstrate the need for preconditioned NRBC, by computing the test case with an inconsistent setup, i.e. using the preconditioned solver with non-preconditioned NRBC. Then, we perform the same computations with a consistent setup. i.e. using the preconditioned solver with preconditioned NRBC.

The results of the computations are summarized in table 1. With the non-preconditioned NRBC setup, the computations are unstable. The vorticity wave and the entropy wave crash after only a few time steps. The acoustic configuration does not crash, but it also does not convergence either. Here, the L1-norm of the residual did not converge further than 8×10^{-3}. In contrast, with preconditioned NRBCs the computations converged for all three wave configurations down to an L1-residual of approximately 5×10^{-12}.

Figure 1 shows the zeroth harmonic of the pressure and the real part of the first harmonic of the pressure for the acoustic wave computation with non-preconditioned NRBC. Since the flow is inviscid, the average pressure represented by the zeroth harmonic, should correspond to the

pressure prescribed at the outlet. However, the average pressure is only 99 336 Pa, showing that the non-preconditioned NRBC does not enforce the correct boundary values in a preconditioned computations.

Regarding the first harmonic, the amplitude of the acoustic wave corresponds to the prescribed 100 Pa, but the wave is distorted by spurious reflections. The reflections produced at the outlet of the domain can be quantified by using a reflection coefficient, which is defined as the ratio of the upstream acoustic mode to the downstream acoustic mode at the interface.

$$c_r = \frac{|\hat{q}|_{\omega,l,5}}{|\hat{q}|_{\omega,l,4}} \tag{37}$$

For the non-preconditioned outlet boundary, the reflection coefficient is $c_r = 0.06$. In other words, 6 % of the prescribed downstream wave is reflected.

Analogously, Figure 2 shows the solution of the zeroth and first harmonic for the acoustic wave computation with preconditioned NRBCs. Here, the correct boundary value of 99 990 Pa is maintained inside the domain. Regarding the first harmonic, the prescribed acoustic wave exits the domain without producing reflections at the outlet. The reflection coefficient of the preconditioned boundary is only $c_r = 3 \times 10^{-6}$.

Similarly good results are achieved with the preconditioned NRBC for the entropy and the vorticity waves, as presented in figure 3. Here, both waves exits the domain without producing reflections, showing that the preconditioned NRBC has good non-reflecting properties for all three presented wave configurations.

6 CONCLUSION

This paper is a first step towards the application of the low Mach preconditioned HB method for internal flow computations. First, low Mach preconditioning was explained and the precondi-

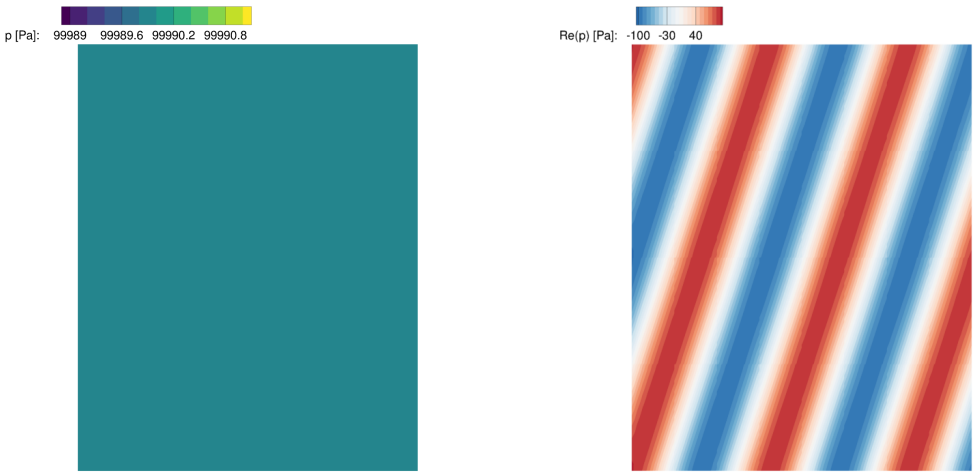

(a) zeroth harmonic (b) first harmonic

Figure 2: Solution for an acoustic wave computed with the preconditioned HB solver with preconditioned NRBC.

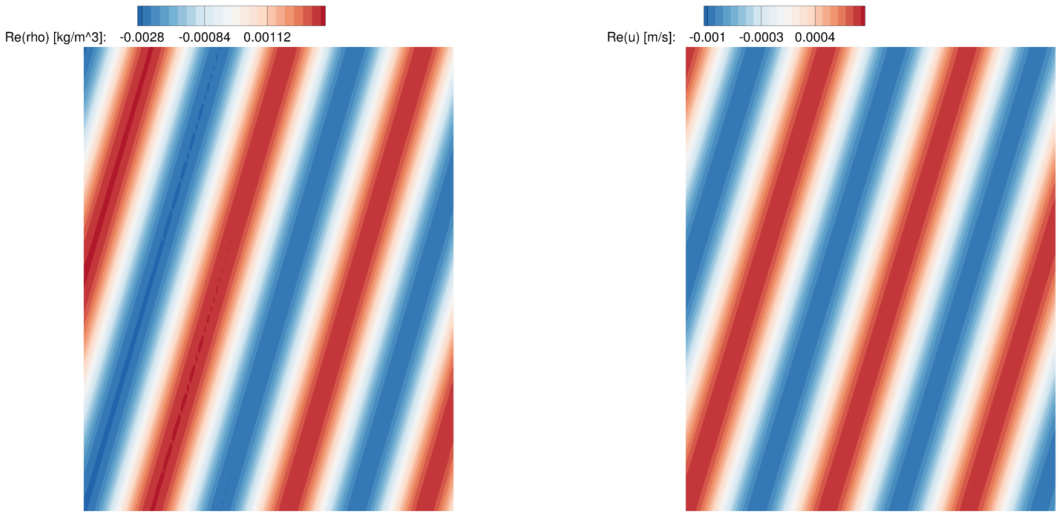

(a) entropy mode (b) vorticity mode

Figure 3: Real part of the first harmonic of the solution for an entropy wave and a vorticity wave computed with the preconditioned HB solver and preconditioned NRBC.

tioned HB solver was presented. Then, the NRBC was preconditioned. While the actual modal non-reflecting boundary condition remains unchanged, the characteristic frame-work needed to ensure that the NRBC is well posed in the pseudo-time must be consistent with the preconditioned governing equations. Therefore, the characteristic framework was reformulated in terms of preconditioned one-dimensional characteristics.

The behavior of NRBCs with and without preconditioning has been tested on a circular duct computed using the preconditioned HB solver. Here, three types of wave were prescribed at the inlet of the domain. The results showed that the non-preconditioned NRBC were unstable, were unable to hold the correct boundary values and lead to strong reflections. Using the preconditioned NRBC greatly improved the stability of the preconditioned computations, while also holding the correct boundary values. Further, the preconditioned NRBC showed good non-reflective properties for acoustic, entropy, and vorticity waves.

REFERENCES

[1] Anker, J. E., Mayer, J. F., and Stetter, H. A preconditioned solution scheme for the computation of compressible flow in turbomachinery at arbitrary Mach number. *Task Quart. 6* (Jan. 2002), 143–176.

[2] Choi, Y.-H., and Merkle, C. The application of preconditioning in viscous flows. *Journal of Computational Physics 105*, 2 (apr 1993), 207–223.

[3] Chorin, A. J. A numerical method for solving incompressible viscous flow problems. *Journal of Computational Physics 2*, 1 (aug 1967), 12–26.

[4] Djeddi, R., Howison, J., and Ekici, K. A fully coupled turbulent low-speed preconditioner for harmonic balance applications. *Aerospace Science and Technology 53* (jun 2016), 22–37.

[5] Frey, C., Ashcroft, G., Kersken, H.-P., and Voigt, C. A Harmonic Balance technique for multistage turbomachinery applications. In *Volume 2B: Turbomachinery* (jun 2014), American Society of Mechanical Engineers.

[6] Giles, M. B. Non-reflecting boundary conditions for the Euler equations. Tech. rep., 1988. CFDL Report 88-1.

[7] Hall, K. C., Thomas, J. P., and Clark, W. S. Computation of unsteady nonlinear flows in cascades using a Harmonic Balance technique. *AIAA Journal 40*, 5 (2002), 879–886.

[8] Howison, J., and Ekici, K. Unsteady analysis of wind turbine flows using the harmonic balance method. In *51st AIAA Aerospace Sciences Meeting including the New Horizons Forum and Aerospace Exposition* (jan 2013), American Institute of Aeronautics and Astronautics.

[9] Kersken, H.-P., Ashcroft, G., Frey, C., Wolfrum, N., and Korte, D. Nonreflecting boundary conditions for aeroelastic analysis in time and frequency domain 3d RANS solvers. In *Volume 2B: Turbomachinery* (jun 2014), American Society of Mechanical Engineers.

[10] Merkle, C. L., and Choi, Y.-H. Computation of low-speed compressible flows with time-marching procedures. *International Journal for Numerical Methods in Engineering 25*, 2 (jun 1988), 293–311.

[11] Potsdam, M., Sankaran, V., and Pandya, S. Unsteady Low Mach Preconditioning with Application to Rotorcraft Flows. vol. 2.

[12] Saxer, A. P., and Giles, M. B. Quasi-three-dimensional nonreflecting boundary conditions for euler equations calculations. *Journal of Propulsion and Power 9*, 2 (mar 1993), 263–271.

[13] Schlüss, D., and Frey, C. Time domain implementation of a spectral non-reflecting boundary condition for unsteady turbomachinery flows. In *24th ISABE Conference* (Mai 2019), Proceedings of the 24th ISABE Conference.

[14] Turkel, E. Preconditioned methods for solving the incompressible and low speed compressible equations. *Journal of Computational Physics 72*, 2 (oct 1987), 277–298.

[15] van Leer, B. Towards the ultimate conservative difference scheme. v. a second-order sequel to godunov's method. *Journal of Computational Physics 32*, 1 (jul 1979), 101–136.

[16] van Leer, B., Lee, W.-T., and Roe, P. *Characteristic time-stepping or local preconditioning of the Euler equations.* 1991.

[17] Venkateswaran, S., and Merkle, C. Dual time-stepping and preconditioning for unsteady computations. In *33rd Aerospace Sciences Meeting and Exhibit* (jan 1995), American Institute of Aeronautics and Astronautics.